ENGINE-OUT TAKEOFF PATH OPTIMIZATION OUT OF TERRAIN CHALLENGING AIRPORTS

Bertrand Masson, Michael Bain, John Page
University of NSW, Sydney, Australia
bmas664@unsw.edu.au; mike@cse.unsw.edu.au; j.page@unsw.edu.au

Keywords: *Takeoff, RNP, Large Aircraft, Engine Out Procedure, Path Planning*

Abstract

Maximum regulated takeoff weights and hence payloads of large commercial jets are limited by Government regulations which take into account local airport conditions as well as a variety of safety factors. One of the challenging conditions that must be met is linked to a minimum obstacle clearance in the unlikely event of an engine failure on the runway at the worst possible time. This requirement becomes an overriding factor for airports surrounded by challenging terrain, and therefore a well defined takeoff path out of these airports has the potential to transform a financially unsustainable operation into a commercially viable one.
The research described in this paper represents an ongoing attempt to resolve this important problem and makes use of recent advances in robot path planning techniques.

Nomenclature

Mnemonic	Description
ARINC	Aeronautical Radio Incorporated
CAS	Calibrated Air Speed
CASA	Civil Aviation Safety Authority (Australia's Aviation Regulator)
EGPWS	Enhanced Ground Proximity Warning System
EOSID	Engine Out Standard Instrument Departure
LOF	Lift-Off Point
MSA	Minimum Safety Altitude
PBN	Performance Based Navigation
PRM	Probabilistic Roadmap
RNP	Required Navigation Performance
RF	Radius to Fix
RTOW	Regulated Takeoff Weight
RWY	Runway
SRTM	Shuttle Radar Topography Mission
TF	Track to Fix
V2	Regulated takeoff safety speed
Vlof	Regulated climb speed at liftoff

2 Introduction

Commercial flights targeting the transport of the general travelling public are highly regulated, and require strict adherence to the Civil Aviation National Regulators. Such agencies define the RTOW which ultimately defines the commercial payload capability that an aircraft can uplift. This RTOW is based on a series of regulations [1][2] that have evolved over many decades of aircraft operations, to protect the travelling public from statistically significant failure cases, notably the failure of the most critical engine at the most critical time. In the event of an engine failure, the climb capability of the aircraft is significantly reduced, and in order to clear terrain/obstacles in accordance with regulatory requirements forces a significant reduction in allowable takeoff weight, and hence payload, particularly in terrain challenging airports.
To regain some of the lost performance due to the engine failure specific paths, also called EOSIDs, may be used in order to avoid the limiting terrain/obstacles. Such paths, however, are usually built manually by highly skilled engineers, and require, in the most limiting case, several iterations on a Full Flight simulator. Turnaround times for difficult airports can be several months, and the outcome may not always be the most optimal path.

In recent times with the advent of high precision guiding GPS equipment on aircraft, these procedures have been tailored to make the best use of aircraft automation which allows set ground tracks and thus allows the operator greater control over the aircraft in avoiding limiting terrain/obstacles.
This possibility, combined with recent advances in robotics path planning [3]-[4] enables the automation of this demanding and expensive task, and will provide airlines the means to further optimize their commercial takeoff limited payloads.
The methods described in this paper represent an ongoing attempt to resolve this important problem.

3 Regulatory Framework

Maximum RTOW is governed by various regulations described in [1] and [2]. Beyond the runway limitations that are independent of local terrain conditions, Local Australian Regulations [1], similar to most international regulations impose two major restrictions on aircraft climb performance assuming engine failure on the runway. The first is related to a minimum climb gradient capability, and the second is related to a minimum obstacle clearance height within a well defined polygon based on the aircraft's intended track.

3.1 Takeoff Segments

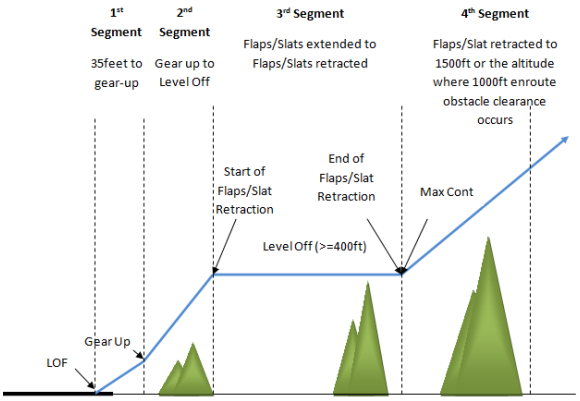

Figure 1 Takeoff Segments

An aircraft must transition from a takeoff aerodynamic configuration to an enroute climb configuration. To achieve this; the climb profile is broken down into four major segments that describe changes in aircraft configuration. These are:

1. First Segment. Commences at 35 feet above the runway and ends when gear retraction is complete. It is assumed that the speed is V2 and one engine has failed and the flaps are in the takeoff configuration. The remaining engines are at takeoff thrust.
2. Second Segment. This segment is from the gear retraction point to the prescribed level-off or acceleration height, which by regulation is not less than 400 feet above the airport reference altitude. In our case, we have set this value to 1500 feet. Takeoff Thrust and flaps/slats remain unchanged.
3. Third or acceleration segment. This segment is dedicated to changing the aerodynamic configuration of the slats/flaps at a fixed altitude, with the end of the segment the point at which all flaps/slats are retracted to the final takeoff climb speed ready for the enroute climb phase. The flap/slat retraction schedule is based on a set of minimum speeds that allow sufficient margin to stall, and assumes a certain time to allow the slats/flaps to mechanically retract. Thrust is maintained to Max Takeoff Thrust levels until the end of the third segment, or a set time, whichever comes first. The third segment must be completed within the time limit on the use of Max Takeoff Thrust which is either 5 or 10 minutes depending certification. Beyond that time, the engine switches to the Max Continuous rating that reduces thrust levels in order to preserve engine life.
4. Fourth or final segment. The aircraft is now in a fully retracted configuration; the thrust schedule is switched to Max Continuous if this has not been done during the third segment. This segment ends once the aircraft clears all terrain within a certain polygon by 1000 feet according to [1], or not less than 1500 feet above the airport. In reality, the

operator will design the end of this segment to be when the aircraft is brought to a safe area at an altitude equal to the MSA.

The above segments are shown in Fig. 1

3.2 Minimum Climb Gradients

In order to provide a safe margin, regulations [1][2] require that the actual aircraft flight path, also referred to as the gross flight path, is lowered by a regulatory decrement of 0.8% for twin engine aircraft, and 1% for quads.
The resulting net flight path must meet at least the minimum climb gradients:

Segment	Twin Engine	Quad Engine
1	> 0%	> 0.5%
2	> 2.4%	> 3.0%
3	> 0%	> 0%
4	> 1.2% at start	> 1.7% at start

Minimum climb gradients are essentially a function of airport altitude and temperature on the day as well as the bank angle of the aircraft.

3.3 Takeoff Cone

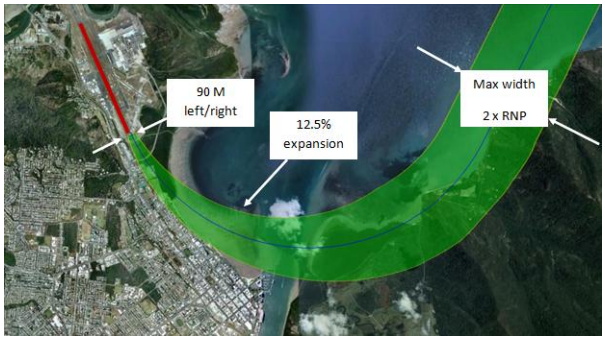

Figure 2 Takeoff Cone definition

Obstacle Clearance is based on clearing obstacles contained in what is referred to as a takeoff cone, or polygon, centered on the intended track of the aircraft. Here lies the crux of the problem since a carefully designed intended track, or flight path, allows minimum obstacle capture and hence the obstacle clearance required RTOW is higher.

The takeoff cone is set by regulations as shown in Fig. 2 to a maximum of 900m lateral offset on a turning track, or to the maximum level of accuracy of the combined Flight Management Computer and GPS constellation (RNP value). For straight tracks, this value can be reduced to a maximum of 600m either side, or to the value of the RNP. Modern aircraft are certified to automatically follow a set track on the ground in what is referred to as a PBN track. This allows a lowering of the lateral offset up to a minimum value of 0.1NM for the most capable systems, thus reducing the amount of terrain captured in the takeoff cone. This RNP value, usually noted RNPx, where x is the radius of the 95% probability sphere where the aircraft will be present. For instance, RNP0.3 means that there is a 95% chance that the aircraft will not deviate by more than 0.3NM, or 555.6m from the intended flight track.

3.4 Obstacle Clearance

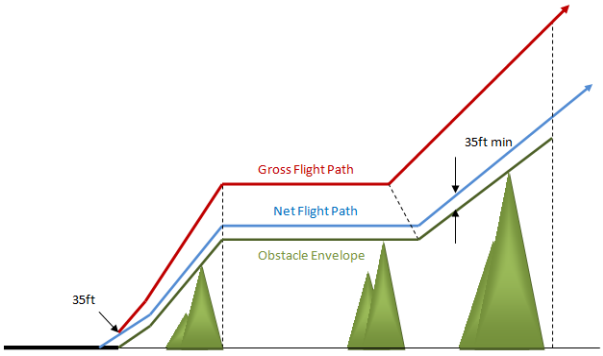

Figure 3: Obstacle Clearance

The resulting net flight path defined in §3.2 must clear all obstacles contained in the Takeoff Cone by at least 35 feet when the runway is considered dry, and 15 feet when the runway is considered wet. This clearance is increased by 50 feet or half the wingspan, whatever is larger, if the aircraft is required to change heading after takeoff.
RTOW is lowered until the both the minimum climb gradient and the obstacle clearance requirements are satisfied.

3.5 Other Considerations

Beyond the minimum regulatory requirements as described in the previous section, a procedure designer may also consider the following:

1. As in standard all-engine approach RNP procedures, do not allow the intended flight path to come within 2 x RNP of terrain.
2. Avoid EGPWS Flight Deck effects by carefully designing the procedure to avoid rapidly increasing terrain. In a manual procedure design, this process is extremely iterative and requires numerous checks with the full flight simulator.
3. Opt for a path that overflies the least amount of terrain.
4. Avoid crossing parallel runways.
5. Avoid restricted areas.

4 Methodology

4.1 Introduction

Previous research conducted by the authors [6] was centered around finding the best path from the runway to a specific point in space using exploration trees based on a combination of arcs and straight lines. These segments, referred to as RF (arcs) and TF (straight lines) were expanded until the target point was met, or when a line of sight was possible between the aircraft and the target point. Although this method was successful in finding a unique path, it was based on a simple constant climb gradient rather than modeling the various takeoff segments, and only allowed a single path calculation.

An operator, however, may want to choose the best target point based on a set criterion, for instance one where minimum fuel is required, or one that reaches the MSA in the shortest amount of time. In order to allow for such an analysis, a method must be developed that allows a path to be computed between the runway end to *any* point at MSA.

The method we have designed is based on sampling the search space in a quasi-random fashion, referred to as the Probabilistic Road Map or PRM. The underlying terrain is extracted from the SRTM [5] 3 arc-second data and runway geographical location, and dimensions are based on publicly available data.

4.2 Algorithm

The complete procedure path build is as follows:

1. Compute climb limited weight
2. Find minimum area around the airport that allows clearance of 1000ft of all terrain based on the above computed weight.
3. Cut the search space in ever increasing areas.
4. Loop until *n* paths reach MSA or all nodes have been explored
5. For each area

Do

6. Sample search space by random selection in the free space. Free space is defined as the space void of all terrain and restricted areas.
7. The *k* nearest neighbours are selected for a given point and linked via an edge.
8. For each edge
    a. Compute aircraft performance data.
    b. Generate a sequence of RF and TF legs.
    c. Extract terrain based on regulatory takeoff cone.
    d. Leg is possible if
        i. Regulatory requirements are met AND
        ii. No EGPWS warnings AND
        iii. Aircraft overflies un cluttered terrain based on a given metric AND
        iv. Path centerline is at least 2xRNP of terrain.
    e. Validate edge

9. Perform a search using Dijkstra's single-source shortest-path algorithm with a cost function based on a combination of distance and terrain density.
10. Purge all points unsuccessful in the Dijkstra search.

While successful points < *x*% generated points.

The resulting paths are stored in appropriate data structures and serialized on disk. As this is a multi-query approach where all paths are pre-computed off-line, paths can be extracted on the fly from the stored data structure so path rendition and obstacle generation is immediate.

4.3 Recursive Random Sampling

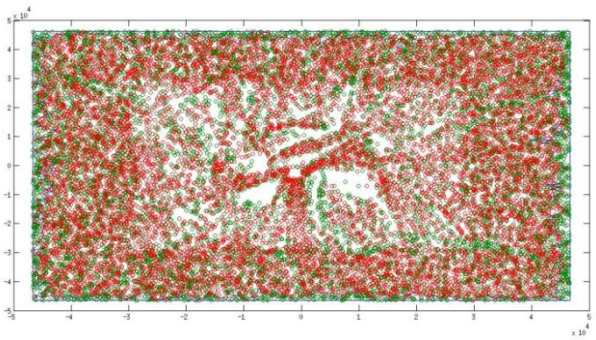

Figure 4 Example of recursive random sampling for Linzhi RWY23, Tibet, China

Although only the x and y components of the three dimensional points are used during the Disjktra search, the z component controls if the point is considered in the free space or not, that is, it is not contained within the terrain or restricted areas. This allows a proper sampling of the free space close to the ground where the effect of terrain is greatest. As the aircraft increases in altitude the likelihood of joining two points via a RF/TF leg increases, and thus the high sampling rate is not required.

The algorithm, for a given area, refines the previous sampling by restricting the search space to the outer contour of the previously successful points. Once a sufficient amount of successful points are generated, the area is then expanded and the process is repeated again.

Fig. 4 shows an example of low density sampling (< 20K) for the high altitude airport of Linzhi. Red points are successful points; green points are the initial samples for the iteration.

If restricted areas are enforced, the sampling will not occur within these areas, nor will any path be allowed to traverse such areas. This is quite easily modeled by defining these restricted areas as polygons; however some interaction may occur between the slicing and these restricted areas as a minimum amount of points must be generated inside each slice for the sampling to be successful.

4.4 Performance Model

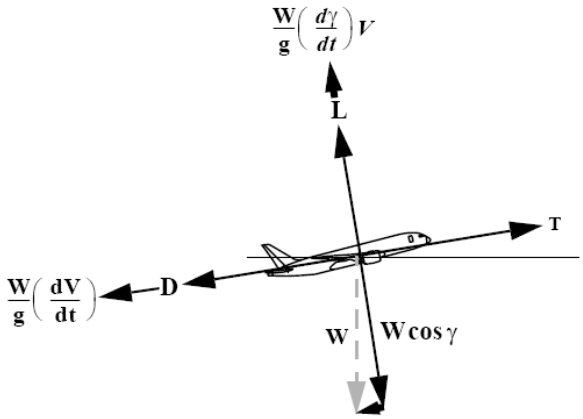

Figure 5 Aircraft Forces [7]

Given the regulatory constraints described earlier, an instantaneous climb angle is computed using the following equation based on the representation of Fig. 5:

$$\gamma = \sin^{-1}\left[\frac{\frac{T}{W} - \frac{C_D}{C_L}}{1 + \frac{V}{g}\frac{dV}{dh}}\right] \text{ [7]}$$

Where:

C_D is the drag coefficient resulting from airframe drag, windmilling drag due to the failed engine, control drag due to the adverse yaw, and finally the drag resulting from the required increase in lift during a turn.

C_L is the lift coefficient

T is the thrust value

W is the instantaneous weight based on the difference between initial takeoff weight and fuel burn.

V is the True Airspeed value

h is the aircraft height

g is the earth's acceleration

All the above values are either computed or a contained in look up tables based on an arbitrary step.

When the aircraft is required to bank, only the projected lift on the vertical axis is used to counteract the weight, therefore the lift needs to increase by a factor of $\frac{1}{\cos\phi}$, see Fig. 6. This in turn increases the drag as a result of the increase in lift.

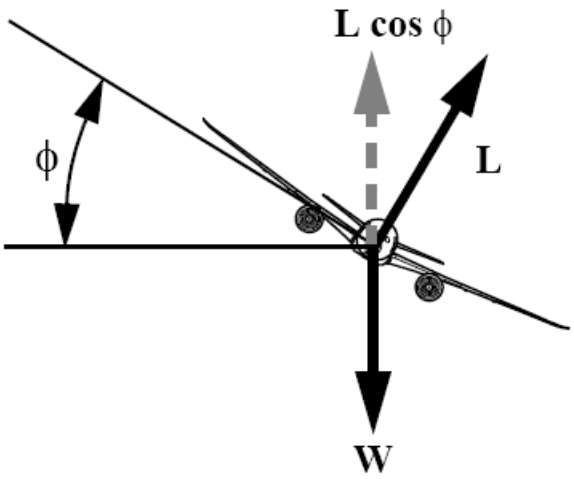

Figure 6 Forces acting on aircraft in a turn [7]

The aircraft net path is computed using the above equation, and subtracting the regulatory pad. Thrust, fuel burn and aerodynamic characteristics are based on the various flap/slat and gear positions. The aircraft modeled in this study is a typical single aisle large jet.

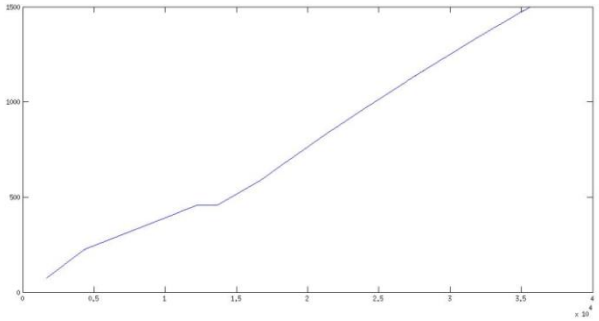

Figure 7 Example aircraft net flight path

4.5 Elementary Leg

Each randomly generated point is connected via a joint RF and TF leg. Due to the fact that a realistic path must be preserved, the initial tangent of the arc is provided from the previous leg. This is the reason why the RF/TF leg generation must be built inside the Dijsktra search as previous legs are not known a priori.

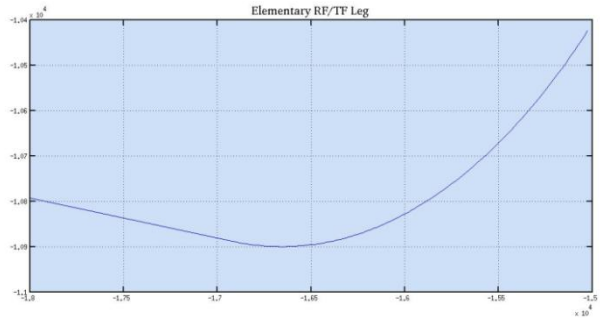

Figure 8 Example combined RF/TF leg

The turn is assumed coordinated, with the radius a function of instantaneous speed and bank angle:

$$R = \frac{V^2}{g \times tan\varphi}$$

Where:

V = True airspeed

g = Earth's acceleration

φ = Bank angle, limited to 15 degrees.

Further work will need to be carried out in order to take into account un-coordinated turns that result from the position of the in-operative engine.

4.6 Terrain Extraction

The terrain is based on the SRTM 3 arc second data distributed by [5]. Only terrain contained in the takeoff cone is used.

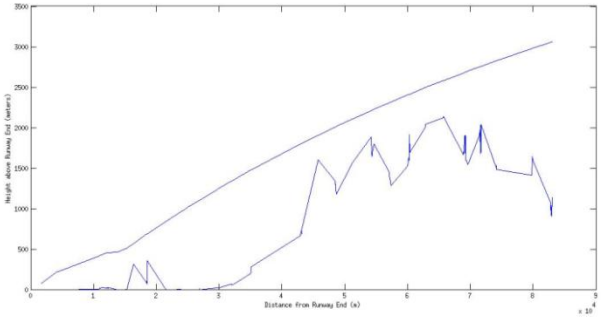

Figure 9 Example of a terrain profile and aircraft net path.

A terrain density function is also computed as a function of 3D position. This density function provides a metric of free space around any point in free space and is based on the size of the maximum square around any given point. The maximum square size is based on the distance from the current point to the closest obstacle. The density value will be used as a component to the cost of traversing an edge. Fig. 10 provides an example for RWY 15 at the airport of Cairns in Queensland, Australia.

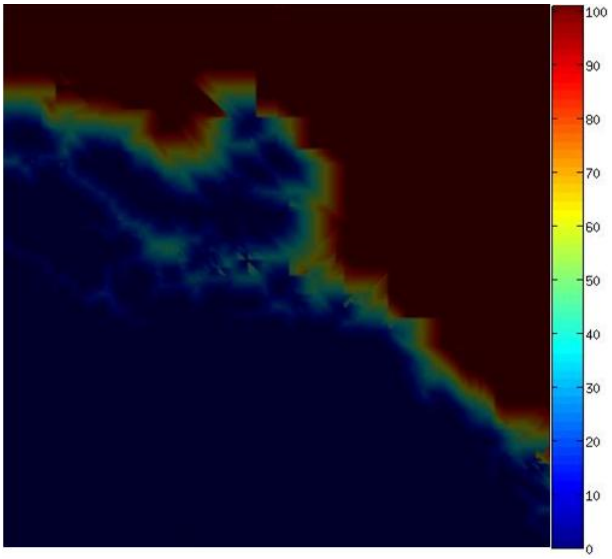

Figure 10 Example of the density function at a given altitude for Cairns, Queensland. Here, the density function maximum is set to 100. Red denotes low density terrain – in this case water.

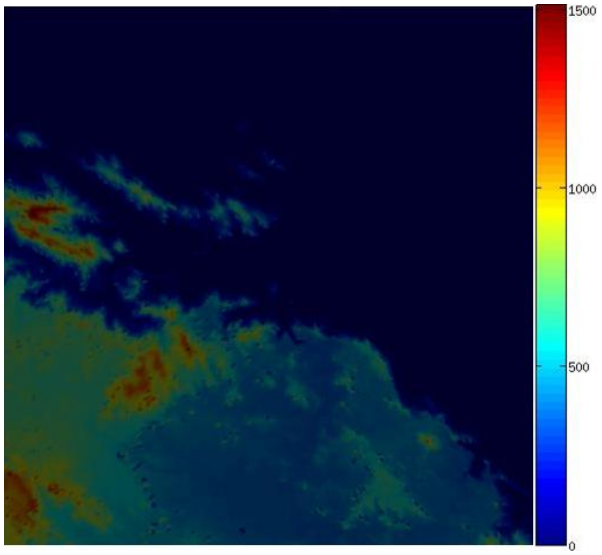

Figure 11 Corresponding terrain map for RWY 15 Cairns, Queensland

4.7 Dijkstra Search

Most PRMs are based on three dimensional physical space. In our case, our network is non Markovian since the previous leg in the search will dictate boundary conditions for the ongoing leg, including values of speed, flap, slat, gear position, it is impossible to join two 3d geometrical points. Therefore, to avoid this issue, the Dijkstra search [8] algorithm is modified to allow the z component of any edge intercepting the (x,y) point to freely float based on the exact aircraft performance. For instance, a single (x,y) pair that represents a point at airport altitude may result in numerous different z values corresponding to aircraft altitude at that point. Furthermore, as the aircraft climb capability is reduced with an engine failure, each physical (x,y) point is allowed to have n nodes, therefore a physical (x,y) point may be visited n times until such a time that a required number of resulting successful paths reach MSA, see Fig. 12.

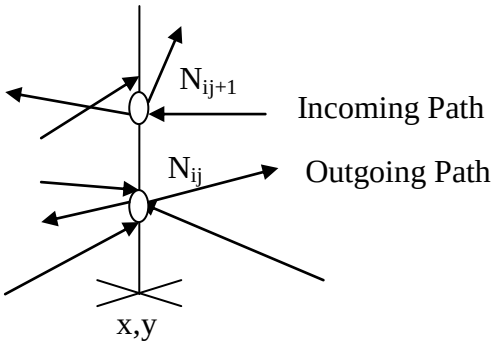

Figure 12 Multi-Layered Disjktra search.

5 Case Study: Linzhi, Runway 23, Tibet, China

5.1 Description

A study was carried out on what is considered as one of the most difficult airports for commercial operations in the world: the high altitude high terrain airport of Nyngchi, Linzhi in Tibet, China. The terrain elevation at this airport is over 9600ft, with surrounding terrain over 18000 ft

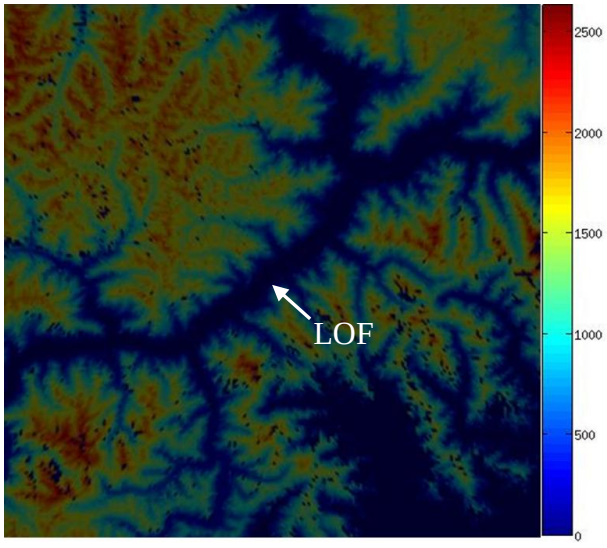

.

Figure 13 Relative terrain height vs. LOF point. Values are in meters.

Areas in Fig 11 shown in blue are at or below the LOF of Runway 23.

For this study, the following parameters were used:

Runway Id: 23
Initial amount of random points: 50000
Number of levels: 1
Number of random points after purge: 33747
Assumed takeoff weight: 46309kg
Speed at LOF: 133kts
RNP half-corridor width: 0.1NM

5.2 Results

From of a total of 50000 initial points, 33747 possible paths were found, which represents a success rate of approximately 67%. This success rate could be improved to 100% if a sufficient number of levels were allowed in the search, although computation time would increase significantly.
Figs 14-20 provide a snapshot of the overall results. Fig 14 provide the complete traces of all the paths generated, with Figs 14&15 showing three of the 33747 paths plotted using Google Earth.

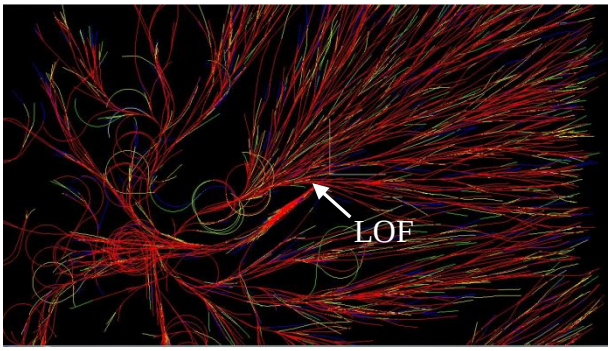

Figure 14 Generated Paths

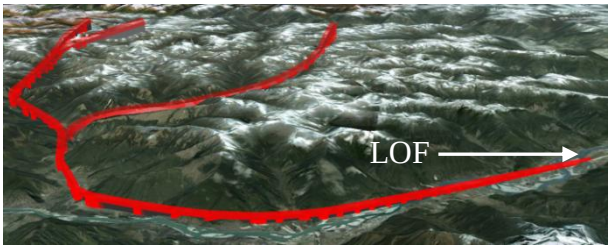

Figure 15 Example of three paths in Google Earth

Figure 16 Detail of Turn

5.3 Discussion

The shaded maps depicted in Figs 17-20 are based on extracting individual scalars such as fuel and distance at the end points of any successful path. As such, they represent interpolated values between successful path end points.

Fig 17 depicts the relative height of the aircraft vs. the highest peak in the studied area. This peak is 17571 feet, and the maximum aircraft height is at 20300 feet.

The area in dark blue denotes an area where the aircraft has exceeded the highest peak, and therefore is able to gain MSA without any hindrance from terrain. In this case, a Dijkstra with a single level suffices to bring the aircraft to MSA given the extent of the blue area. If another level were to be added, then the contour map would be of a constant blue value denoting that all points can reach MSA.

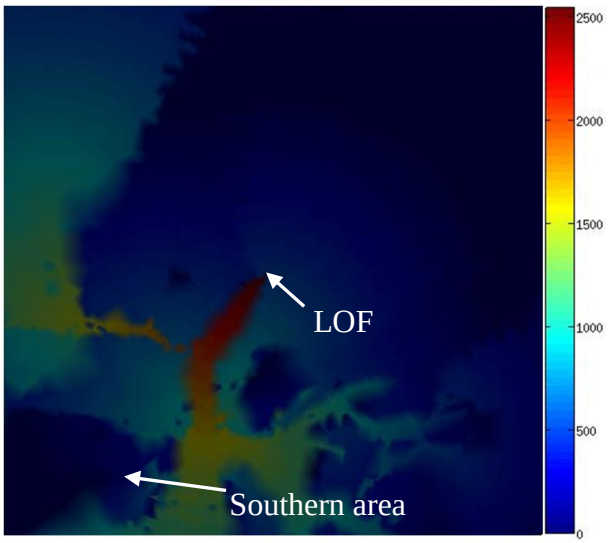

Figure 17 Highest Terrain – Aircraft altitude (ft)

Fuel used and accumulated distance depicted in Figs 18 and 19 are in fact only slightly scaled by the near constant fuel flow and difference in speed. It is interesting to note that the southern area shown in Fig 17 has a dark blue area even though it is quite close to the LOF point. This is due to the fact that the search has created a circling path to allow the aircraft to gain height.

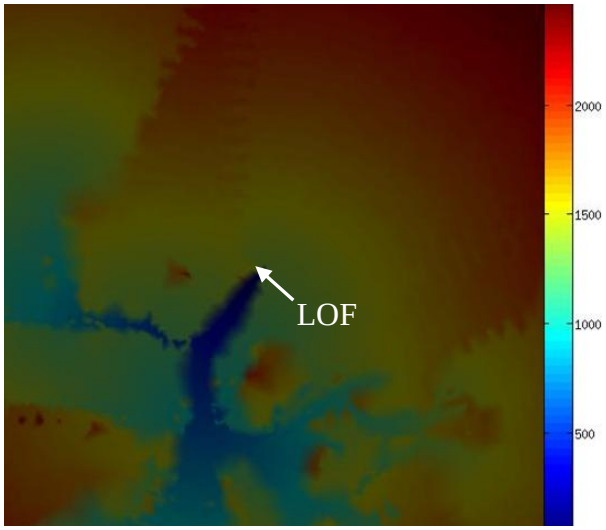

Figure 18 Fuel used (kgs)

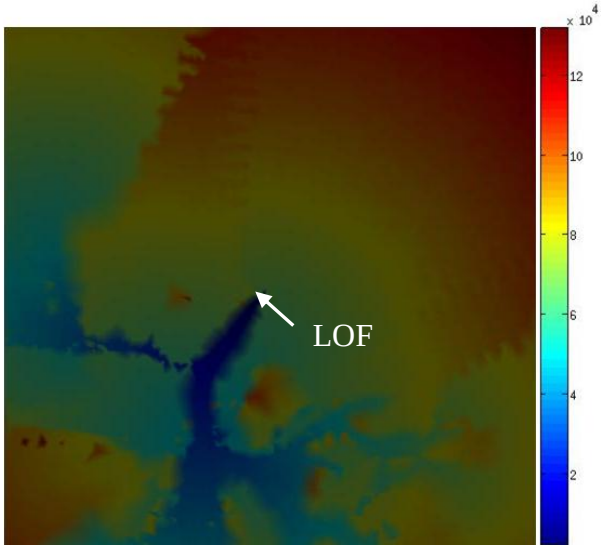

Figure 19 Accumulated Distance from LOF (m)

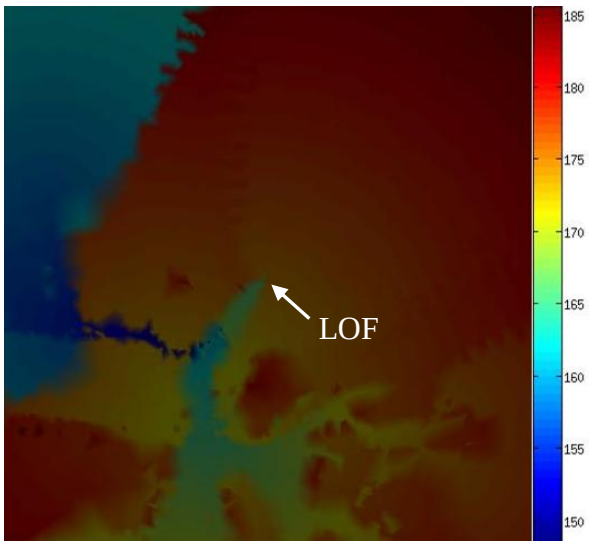

Figure 20 Speed (KTAS)

6 Conclusion

The method of a strongly coupled sampling based method, an optimal search algorithm and a regulatory-compliant aircraft performance model has yielded promising initial results as it is able to produce a high number of successful paths that meet the regulatory constraints. More importantly, a reasonable payload is uplifted from the airfield and escape paths can be rapidly prototyped without lengthy manual construction. It also allows the depiction of shaded maps which provide a very good understanding of the interaction of aircraft performance limitations when operating in terrain challenging airports. Finally, as the analysis is carried out offline, and the path query can be carried out online, this will allow a tight integration of the takeoff performance and path extraction in a time critical case.

The next steps of this research will be to carry out a systematic evaluation of the method on a sample set of runways and compute actual takeoff performances. A wind model will then also be integrated in order to capture the effect of wind gusts. Finally, the combined all engine-engine out case will be studied in order to properly define branch points to cover the case when the engine fails during a standard all engine climb.

References

[1] Australian Government, Civil Aviation Safety Authority. "*Civil Aviation Order 20.7.1B*". Civil Aviation Safety Authority, Canberra

[2] Australian Government Civil Aviation Safety Authority. "*Civil Guidelines for the Consideration and Design of: Engine Out SID (EOSID) and Engine Out Missed Approach Procedures*". Civil Aviation Safety Authority, CAAP 235-4(0) November 2006

[3] S Karaman, E Frazzoli, "*Sampling-based algorithms for optimal motion planning*". The International Journal of Robotics Research 2011 30:846, June 22 2011

[4] H Choset, K M. Lynch, S Hutchinson, G Kantor, W Burgard, L E. Kavraki, S Thrun. "*Principles of Robot Motion, Theory, Algorithms, and Implementations*". The MIT Press (2005)

[5] Jet Propulsion Laboratory. "*Shuttle Radar Topography Mission*". http://www2.jpl.nasa.gov/srtm/ [cited 23rd of June 2012]

[6] B Masson, M Bain, J Page. "*Engine-Out Takeoff Path Optimization out of Terrain Challenging Airports*". presented at AIAA Guidance and Navigation Control, Portland, Oregon, USA, 8-11 August 2011.

[7] W. Blake, Performance Training Group. "*Jet Transport Performance Methods*". Boeing Commercial Airplanes, Boeing Document D6-1420, March 2009

[8] Cormen, Leiserson, Rivest and Stein. "*Introduction To Algorithms*". (2nd Edition) MIT Press, Cambridge, MA. (2001)

Copyright Statement